Sensors and Actuators A 302 (2020) 111825

Contents lists available at ScienceDirect

Sensors and Actuators A: Physical

journal homepage: www.elsevier.com/locate/sna

Reliable Tin dioxide based nanowire networks as ultraviolet solar radiation sensors

Estácio P. de Araújo*, Adryelle N. Arantes, Ivani M. Costa, Adenilson J. Chiquito

NanOLaB, Departamento de Física, Universidade Federal de São Carlos, Rodovia Washington Luiz, Km 235, Monjolinho, 13565-905, São Carlos, São Paulo, Brasil

ARTICLE INFO

Article history:
Received 29 October 2019
Received in revised form 6 December 2019
Accepted 27 December 2019
Available online 28 December 2019

Keywords:
Tin dioxide nanowire network
UV sensor
Solar radiation

ABSTRACT

Nowadays, 1D material SnO_2 (n-type) have been standing out, demonstrating their potential application in ultraviolet (UV) radiation and chemical sensing, as in optical communication, safety devices and biological fields. In this work, we discuss the characteristics of an UV sensor device built in a metal-semiconductor-metal (MSM) architecture using a SnO_2 nanowire network as the sensing element. SEM and XRD techniques were used to characterize the device, revealing uniform structures and excellent crystallization, respectively. Photoresponse of the nanowire network was obtained under three different sources of radiation: one in the visible region (White Light- 9.5 mW/cm^2), another in the UV region (UV Lamp – 2 mW/cm^2) and finally, using direct solar radiation (Sun Light – 78.6 mW/cm^2). The area illuminated of device was 7.8×10^{-7} m^2.When exposed to the sources containing UV wavelength, we obtained a current on/off ratio of the order of 10^4, rise time up to 2.8 s and multiple decay times from 1 s to 100 s. These results enable the design of a sensor based on nanowire networks presenting high sensibility and selectivity, particularly in outdoor measurements and also an optimized regime of operation.

1. Introduction

Due to the necessity of establishing reliable parameters that determine the benefits and risks of ultraviolet (UV) radiation exposure, the study and development of UV photodetectors has extended beyond its usual applications in optical communication and flame detectors, gaining attention in the hospital environment and as exposure sensors [1]. Regarding exposure control, it is common to find recommendations that take into account data extracted from North America, Europe and specific South American regions [2–4], so as to disregard key criteria related to geographic location, resulting in low reliability of the data. Hence, the need to establish methods for calculating, for each region, the benefits and risks to human health, drives the research and development of rapid, high-sensitivity and portable devices [1] that provide real data from the investigated environment.

Solar radiation spectrum includes a band of electromagnetic radiation with a wavelength range of 100–700 nm, consisting of UV radiation (energy distribution range of 3.1–12.4 eV) and the visible (VIS) region. The UV region can be divided into the following bands: UV–C (100–280 nm) that is strongly absorbed by the ozone layer, UV–B (280–320 nm) and UV–A (320–400 nm), which reach the surface and interact with matter. Within this wide range it is indispensable to obtain devices that facilitate the monitoring of radiation reaching the surface. In terms of meteorological services, each parameter requires different equipment: for example, heliographs are used to acquire the insolation level, pyranometers to obtain the solar flux density, solar pyrometers and pyro-heliometers to measure diffuse and direct radiation, respectively [4]. However, due to nanotechnology development it is now possible to obtain all these parameters using only a single semiconductor device that acts as a photodetector for instance, demonstrating the enormous potential of nanostructured semiconductors and stimulating the study and research in this field [5].

Several UV photodetector prototypes have been recently proposed, composed by GaN, ZnS, NiO, ZnO, TiO_2 among others [6–9], all wide bandgap semiconductor materials. In addition, many properties are optimized when used as one-dimensional nanostructures, such as nanowires, which increase photosensitivity, achieve good resolution at a specific wavelength, provide fast response time to the device and operate under low voltage conditions [1,6,10]. Furthermore, when using a nanowire it is possible to notice advantages in comparison to bulk materials. The large surface area to volume ratio increases the influence of surface states in the electric current inside the nanowire, leading to a more effective conduction in the transport channel [10]. These surface states

* Correspoding author.
E-mail address: estacio.paiva@gmail.com (E.P. de Araújo).

https://doi.org/10.1016/j.sna.2019.111825
0924-4247/

originate during the nanowire growth process and, in the class of metal oxides such as SnO_2, are related to the oxygen vacancies that become the basis of device operation [11].

Tin dioxide is an n-type semiconductor oxide with a wide bandgap around 3.6 eV at room temperature. It has proven to be an efficient material for the construction of UV photodetectors, among other devices [12–16]. In one-dimensional scale, it is possible to obtain structures with well-defined morphologies, for example, nanowhiskers, nanobelts, nanorods and nanowires [11,13,14,17,18], enhancing their applicability in the scope of sensitivity. SnO_2 based UV photodetector studies report rise (τ_r) and decay time values (τ_1 and τ_2), on/off current ratios at varying operating voltages for devices built with different architectures and manufacturing methods [12,19–21]. For a single nanowire sensor, Haiping Shi et al. have reported an on/off rate of 10^2 at a 20 V operating voltage, rise time of 0.4 s and decay time of 0.6 s, using 335 nm excitation wavelength [19]. Junebeom Han et al. have conducted a study using UV Lamp (351 nm), resulting in multiple decays with values of 8.9/2.0 s (τ_1/τ_2) for a nanowire network device built by the spray method on a flexible substrate [21]. For a nanowire network synthesized by the same VLS mechanism used in our work, Jyh and Cheng have reported an on/off ratio of approximately 2 operating at 12 V for UV Lamp (365 nm), with τ_r and τ_1 greater than 50 s and 150 s, respectively [12].

In addition to the simplicity of fabricating the device with a nanowire network, during the synthesis process numerous junctions are formed between nanowires that give rise to potential barriers. These potential barriers associated to the potential redistribution at the interfaces dominate the transport processes at the junctions, being affected (and modulated) under UV radiation [22], resulting in significant changes of electrical conductivity.

In this work, we discuss the characteristics of an UV sensor device based on a SnO_2 nanowire network when under three different sources of radiation: one in the VIS region (White Light), another in the UV region (UV Lamp) and finally, using direct solar radiation (Sun Light). The electrical characterization techniques used, current-voltage (I–V) and current as a function of time (I-t) curves with and without irradiation, enabled the acquisition of fundamental parameters to characterize the photodetector. When exposed to the sources containing UV we accomplished a current on/off ratio of the order of 10^5, rise time up to 2.8 s and decay times less than 1 s ($\tau_1 < 1$ s) and approximately 100 s ($\tau_2 \approx 100$ s). Comparing the data obtained for the source without UV wavelength, the excellent results and the selectivity achieved by the device to this wavelength when using direct solar radiation are highlighted.

2. Materials and methods

Tin dioxide nanowires were synthesized based on the vapor-liquid-solid (VLS) growth method. This mechanism is assisted by metal catalyst nanoparticles that act as preferential sites for the adsorption of vapor components, leading to a guided one-dimensional growth of the nanowire [10,23]. Initially, thin films of gold (15 Å) were deposited (Edwards 306 coating system) in previously prepared Si/SiO_2 substrates (oxide layer 500 nm thick) in order to generate the catalyst nanoparticles. The synthesis was carried out in a tube furnace system (Lindberg Blue M), where a high purity Tin powder (0.1 g, Aldrich, purity > 99.99 %) was placed in an alumina crucible which was positioned at the center of the furnace and heated to 950 °C (heating rate of 18.5 °C/min) and remained at this value for 60 min. For the vapor transport to the synthesis region, an Argon/Oxygen mixture with a constant flow of 20/5 sccm (Mass Flow MKS 1149) was maintained along with controlled pressure by a vacuum pump around 350 mbar. As-synthesized products were then examined by scanning electron microscopy (SEM, JEOL JSM 6510, operated at 20 kV) and X-ray diffraction (XRD, Rigaku D/max-2500, Cu-Kα radiation).

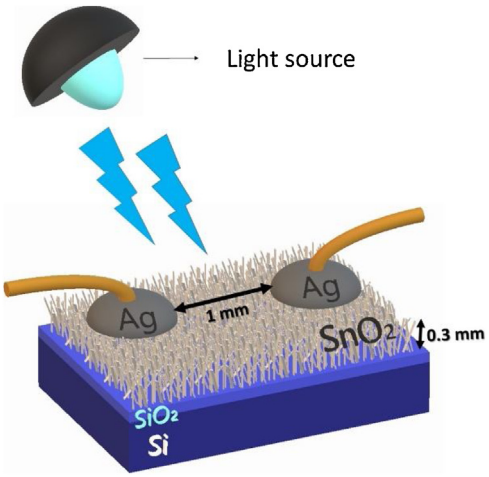

Fig. 1. UV Sensor MSM architecture.

The UV photodetector was built based on a metal-semiconductor-metal (MSM) structure, which consists in a semiconductor material in contact with two metallic electrodes [24]. The semiconductor is the SnO_2 nanowire network whereas the metallic electrodes are the silver paste (Ticon ISO9001), as depicted in Fig.1. The surface density was estimated to be 6.25×10^5 nanowires/mm^2 and the active area effectively exposed of 1 mm^2. Furthermore, there was no need of expensive or complex photolithography processes neither clean room environment. The photoresponse of SnO_2 nanowire network UV photodetector was obtained using an electrometer (Keithley 6517-A) and a chopper to generate the on and off states.

Solar radiation data are commonly supplied by meteorological studies (INPE 2019) and were used to estimate a value to the solar radiation power at the measurement day [2,3]. The position related to the Sun in May 27th at midday (UTC/GMT −3 h) was found to be in an azimuth angle of 22.31° and obtained an AM 2.6 [25]. For this given value, the intensity calculated for the exposed device was of 78.6 mW/cm^2. Obviously, this value is not exact due to global irradiance dependence on direct and diffuse illumination, likewise effects induced by clouds, wind speed, dust and others that are not taken into account.

Beyond Sunlight, two other excitation sources were used: an UV Lamp (Cole-Parmer UVGL-15 - 2 mW/cm^2) with main spectral lines in 254 and 365 nm; a White Light (FOI-150 Techniquip – 9.5 mW/cm^2) coupled to an optical fiber that also acts as an UV filter, resulting only in VIS wavelength. Sunlight measurements were all conducted outdoors with 20 % humidity and temperature of 27 °C, while both artificial sources measurements were performed in controlled environment with humidity and temperature of 59 % and 22 °C, respectively. All measurements were conducted within a scan time of 30 min for each sample. To verify the reproducibility of the devices, a total of five samples grown under the same synthesis conditions were analyzed.

3. Results and discussion

Fig.2(a) depicts the X-ray diffraction pattern (XRD) of as-grown samples. All diffraction peaks indexed show rutile-like peaks (JCPDS 41–1445) [26] as expected for the tetragonal structure of SnO_2 (a = 4.738 Å and c = 3.187 Å) within the $P4_2/mm$ spatial group. A scanning electron microscopy (SEM) image of VLS synthesis is presented in Fig.2(b): structures with lengths of tens of micrometers and cross-section mostly displaying rectangular geometry

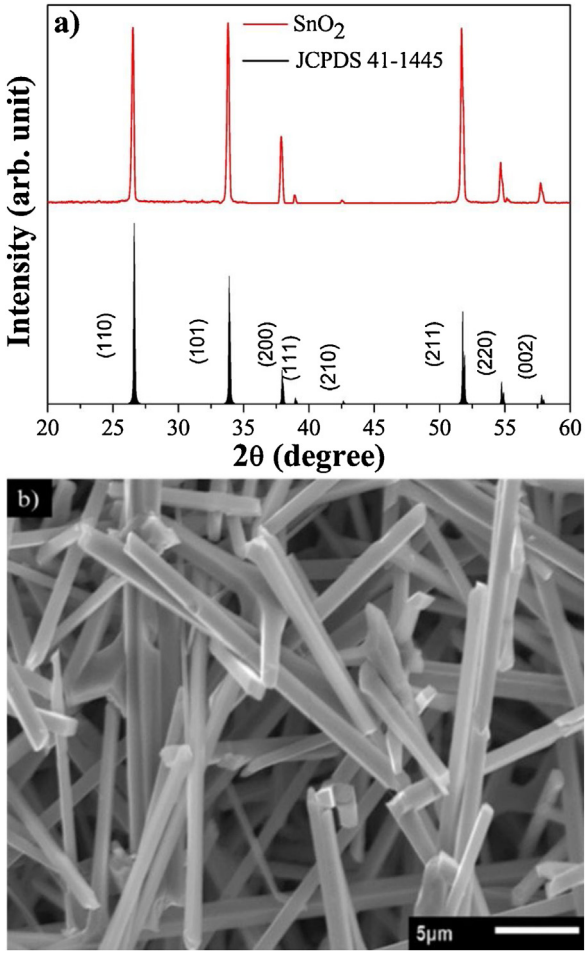

Fig. 2. a) XRD pattern of as-grown samples (red) displaying the rutile like peaks (JCPDS 41–1445, black) b) SEM image of the nanowire network.

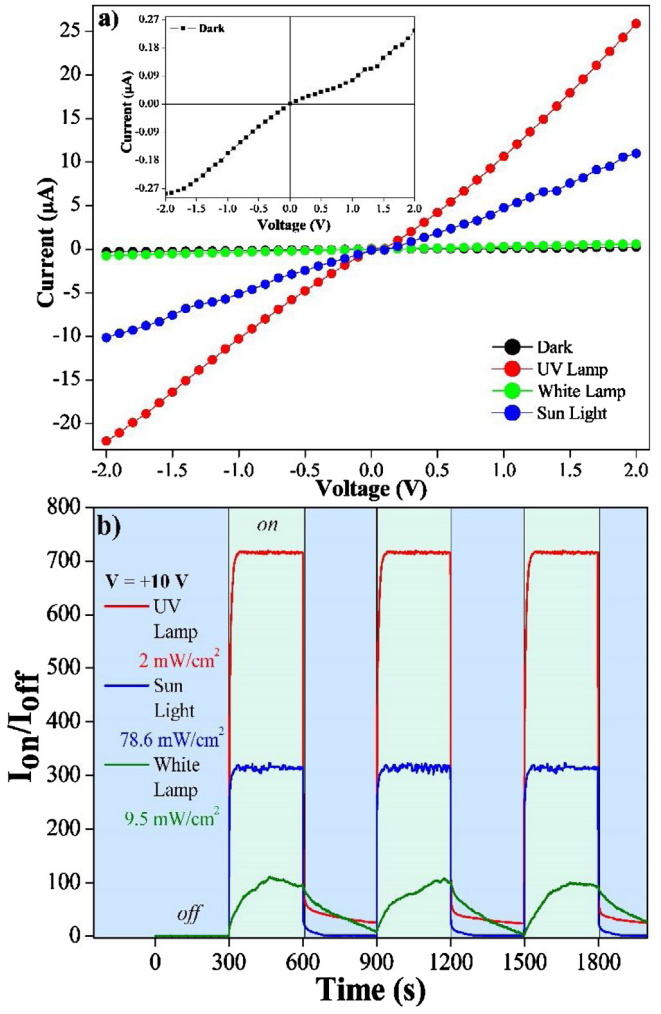

Fig. 3. a) I–V curves of the SnO_2 nanowire network photodetector, highlighting the dark condition behavior in the inset; b) I-t curves comparing different sources and intensity for the same voltage condition.

were observed. Moreover, it is also possible to observe multiple branched nanowires that can arise during the synthesis process of one-dimensional nanostructures, known as self-catalytic dendrites [27], although there is no interference in our results.

I–V curves of SnO_2 nanowire's network device are displayed in Fig.3(a), in dark (black), under Sun light (blue), UV Lamp (red) and White Light (green) conditions. Under illumination, the photoionized charges are activated and space charge regions are modulated, increasing the current and simultaneously provoking a barrier height variation of the metal-semiconductor (MS) interface. Thereby, the curve behavior presents itself as linear; however, linearity does not imply in barrier absence [28], because some effects on the MS interface should be considered when the device is under illumination and in the dark. These properties can be better analyzed in the back-to-back diode model [29].

Fig.3(b) shows the device on/off current ratio as a function of time under three different excitation sources and an operation voltage of 10 V. The photoresponse of the device reaches an on/off ratio (in percentage) up to 10^4 for all sources. The distinct responses to different UV sources are expected and related to the wide range of wavelengths that compose the Sun Light. Furthermore, when both are compared to the White Light, one can see clearly the high sensitivity and selectivity of the device to wavelengths in the UV region. Although the UV portion of the solar spectrum is small, according to geographic and meteorological parameters, the UV indexes for our region during the study period varied from 8 to 11, considered a very high index (8–10) to extreme (≥11) [2]. In addition, the chosen measurement time (12 h UTC/GMT −3 h) provides the conditions under which there is a higher proportion of direct than diffuse radiation.

Since satisfactory results were obtained, other voltage values were investigated in order to compare the device behavior and achieve an optimized operation regime regarding response times and on/off current ratio. Fig.4 displays on/off current ratio in function of time of all sources under different voltages: 10 V, 5 V, 1 V, 0.1 V, -1 V and -10 V.

White Light data are presented in Fig.4(a), where one can notice that due to its excitation range between 1.65 and 3.1 eV, the photocurrent obtained is predominantly originated by the excitation of the levels present inside the energy bandgap. When irradiating only with UV, which has energy equivalent or even greater than the value of the SnO_2 bandgap [Fig.4(b) and (c)], the result is the photocurrent maximization. Differences between positive and negative values for the same voltage can be attributed to different barriers formed at MS junctions [29]. All curves were separately analyzed and rise time (τ_r) and decay times (τ_1 and τ_2) were obtained from experimental data fitting to the following equations:

$$I(t) = I_0(1 - e^{-t/\tau_r}) \quad (1)$$

$$I(t) = I_0 + Ae^{-t/\tau_1} + Be^{-t/\tau_2} \quad (2)$$

in which I_0 is the maximum current (steady state), t is the time, A and B are constants. Fig.5(a) shows the current variation of a device

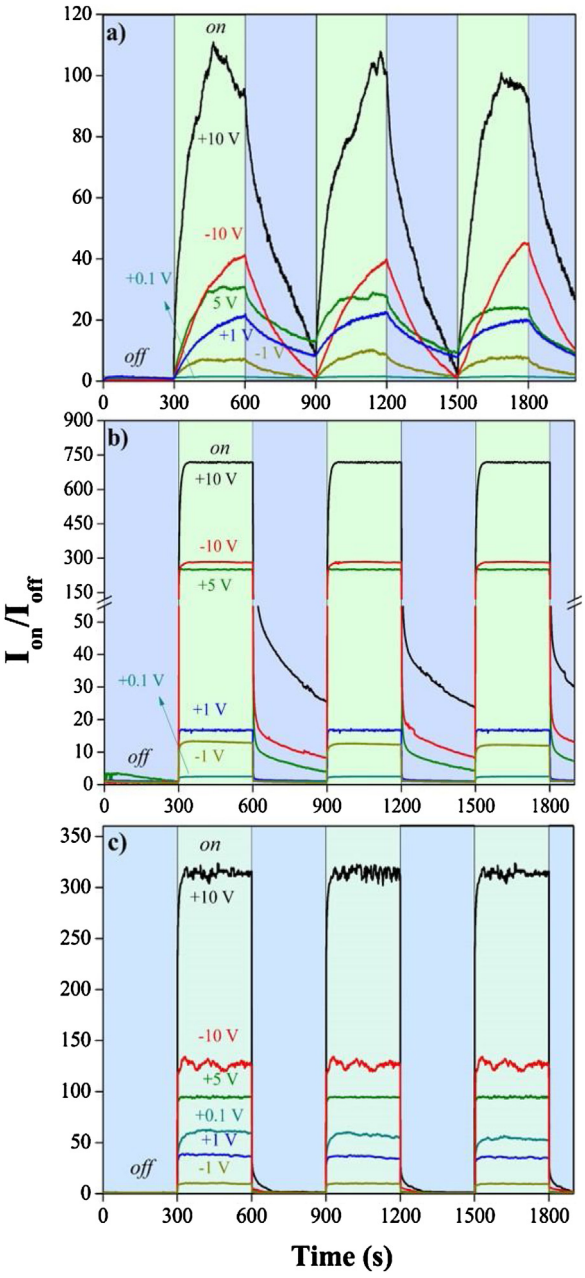

Fig. 4. I-t characteristics of the device when under illumination of a) White Light; b) UV Lamp and c) Sun Light.

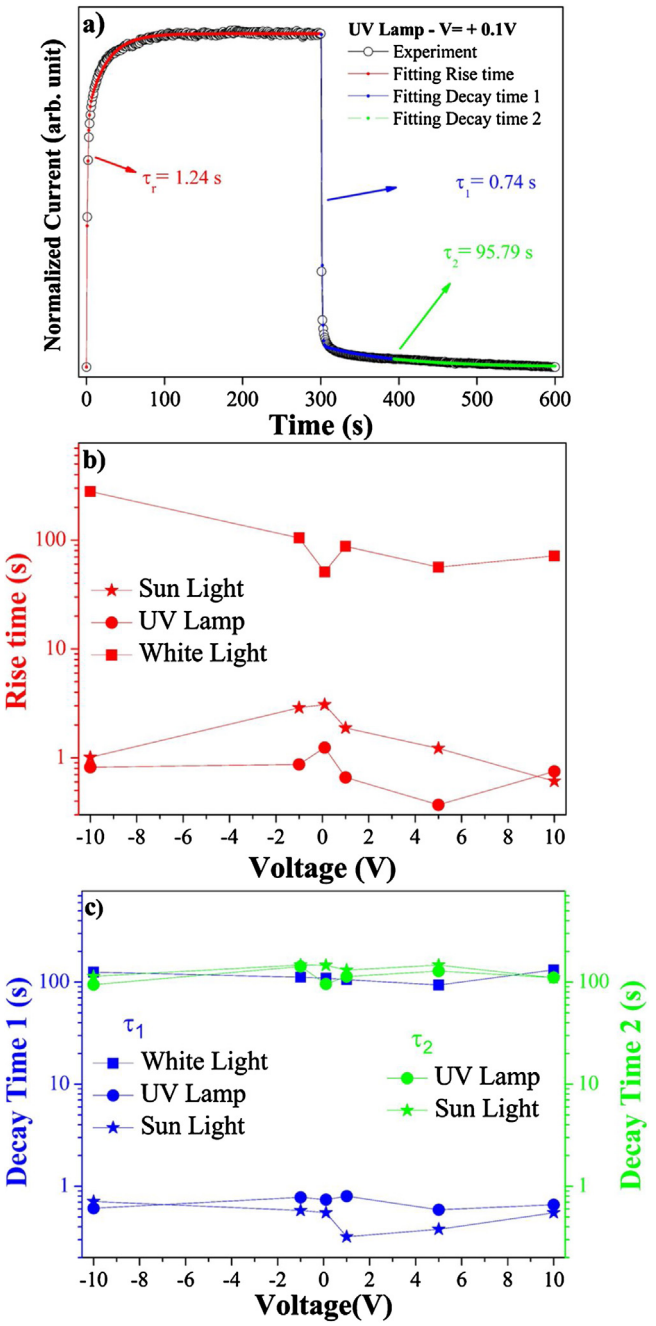

Fig. 5. a) Curve fitting for rise time (τ_r) and multiple decay times (τ_1 e τ_2) for an operating voltage of 0.1 V and under UV Lamp illumination; for all sources under different operating voltages, panel b) displays the rise time and panel c) shows multiple decay times: τ_1 (blue) and τ_2 (green). The error obtained from the analysis is smaller than the size of the curve points.

subjected to a 300 s pulse at a voltage of 0.1 V. Rise time (red) and the values obtained for each voltage can be seen in Fig.5(b). Using an UV Lamp the response time was between 0.3 s and 1.2 s (0.3 s $\leq \tau_r \leq$ 1.2 s); exposing the device to the Sun Light were achieved values close to 0.8 s and 2.8 s (0.8 s $\leq \tau_r \leq$ 2.8 s) whereas for White Light, between 56.3 s and 280 s (56.3 s $\leq \tau_r \leq$ 280 s). Comparing the values of τ_r, the White Light has a significantly longer time, which is an expected effect due to the excitation energy being smaller than the SnO_2 bandgap energy. In addition, it was noted that there is no large variation in τ_r due to different voltage levels. Thus within the fittings' uncertainty ($r^2 = 0.9991$) it is consistent to consider that τ_r is independent of the voltage for all light sources.

Multiple decay times were analyzed using Eq. (2), in which τ_1 is related to the rapid change in charge concentration when irradiation is ceased, while τ_2 refers to trapping and releasing charges due to oxygen vacancies and other levels within the bandgap [25].

One can see the values of τ_1 (blue) in Fig.5(c), where decay times of up to 0.8 s ($\tau_1 \leq$ 0.8 s) were achieved for all values of applied voltages to the sources containing UV radiation. In contrast, all values of τ_1 obtained for White Light exceeded 90 s (93.6 s $\leq \tau_1 \leq$ 131.5 s). The values of τ_2 (green) for the Sun Light and UV Lamp are both around 100 s ($\tau_2 \approx$ 100 s), while the absence of this parameter for White Light. In general, the curve profile and the fittings for the White Light do not allow distinguishing between two types of decay, resulting in only a long current decay time. By comparing the behavior of the three sources, τ_1 can be interpreted as the rapid variation between a state of current saturation and an abrupt drop due to cessation of irradiation [22,30]. Thus, if no current sat-

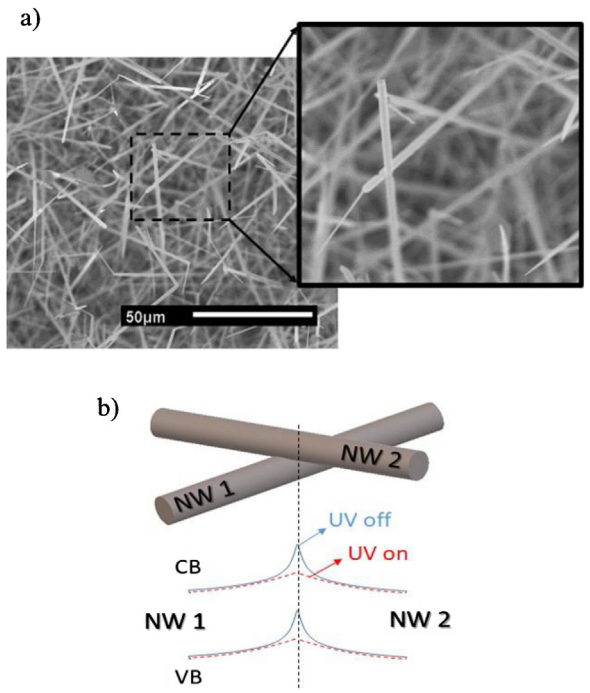

Fig. 6. a) SEM image of nanowire junctions and b) schematic of a junction barrier for the electron transport. CB and VB are the conduction band and valence band, respectively.

uration region is achieved, the decay becomes long and associated with the relaxation processes that occur between the energy levels within the bandgap [24]. Moreover, the time value discrepancy highlights the effect of the absence of UV radiation on decay processes, reinforcing the device's high sensitivity and selectivity to this wavelength.

Basically, all studies conducted in metal-oxide nanostructures carried out to date point out the electronic transport as deeply dependent on the role played by oxygen vacancies. For a single nanowire, surface effects related to oxygen adsorption/desorption and the electron-hole pair dissociation due to the applied voltage take place simultaneously [31]. In the first case, oxygen molecules are adsorbed on the SnO_2 surface by capturing the electrons ($O_{2(gas)} + e^- \rightarrow O^{-2}_{(ads.)}$) and after illumination, some of these photogenerated charges tend to migrate to the nanowire surface to discharge the adsorbed oxygen ion ($O^{-2}_{(ads.)} + h^+ \rightarrow O^{2}_{(gas)}$). In the latter case, there is a conductive channel inside the nanowire and the e–h pair generated due to the absorbed photon is separated by the applied external electric field resulting in an increment of the current.

Regarding the nanowire network studied here, there are a large number of nanowires establishing connections with each other and forming a percolative path for electrical conduction [32]; however, each nanowire has its own geometrical characteristics and electronic properties, randomizing conduction processes. Simultaneously to processes of conduction for a single nanowire, electronic transport in a network is highly dependent on the behavior of the regions where the junctions between nanowires are formed [Fig. 6(a)]. Interface effects then give rise to potential barriers with width and height that can be lowered by UV illumination [Fig. 6(b)], since it provokes an increase of carrier density. Thereby, in the presence of UV illumination, electrons can easily overcome the potential barriers and transport through the network, resulting in a significant increase of current [22].

In brief, the on/off ratio maintained its value in the order of 10^4 for cases in which the device operated in voltages of 5 V and ± 10 V under an UV Lamp illumination, whereas for the Sun Light when operated in ± 10 V and using the White Light, only when operated in 10 V. The rate decreased one order of magnitude under illumination by an UV Lamp, the Sun Light and a White Light when operated in -10 and 5 V, 1 V and ± 1 V, respectively. The remaining values kept the minimum rate of 10^2. In general, sensor optimization was achieved by operating in: 5 V using an UV Lamp (τ_r = 0.37 s, τ_1 = 0.59 s and τ_2 = 128.7 s) and in 10 V for both Sun Light (τ_r = 0.61 s, τ_1 = 0.55 s and τ_2 = 110 s) and White Light (τ_r = 71.6 s and τ_1 = 131.5 s). Our device demonstrated an outstanding UV photoresponse, which can be reinforced when compared to other more complex sensors. For instance, Daeil Kim et al. have achieved na approximate on/off ratio of 10^5 for a device built as a field effect transistor combining a SnO_2 nanowire network with carbon nanotubes, but much longer rise and decay times of 40 s and 10 s, respectively [20]. Regarding response time, Hiping Shi et al. have reported for a SnO_2 single nanowire photodetector under UV illumination (335 nm) rise and decay times ($\tau_r \approx 0.4$ s and $\tau_1 \approx 0.6$ s) very close to the ones obtained for our sensor [19].

4. Conclusion

In summary, SnO_2 nanowire networks were grown from chemical vapor deposition, through VLS mechanism. For device fabrication based on a MSM structure, there was no need of expensive or complex photolithography processes neither clean room environment. Three excitation sources were used to characterize the photodetector: an UV Lamp (2 mW/cm^2) with main spectral lines in 254 and 365 nm; a White Light (9.5 mW/cm^2) coupled to an optical fiber that also acts as an UV filter and the direct Sun light (78.6 mW/cm^2), the area illuminated of device was 7.8×10^{-7} m^2. Optimized regime of the photodetector was achieved by operating in 5 V using an UV Lamp (τ_r = 0.37 s, τ_1 = 0.59 s and τ_2 = 128.7 s) and in 10 V for both Sun Light (τ_r = 0.61 s, τ_1 = 0.55 s and τ_2 = 110 s) and White Light (τ_r = 71.6 s and τ_1 = 131.5 s). The results demonstrated high sensitivity (above 10^4) and selectivity to UV wavelength, emphasized when compared to outdoor measurements. Additionally, we obtained fast response time, stability and reproducibility, all essential features for a quality UV photodetector.

Author statement

All authors contributed equally to this work's development.

Declaration of Competing Interest

The authors declare that there is no conflict of interests.

Acknowledgments

The authors thank the financial support from the Brazilian agencies: Grant Nos. 2013/19692-0, 2013/07296-2, São Paulo Research Foundation (FAPESP) and Grant Nos. 302640/2010-0 and 305615/2014-9 (CNPq).

References

[1] F. Omnès, E. Monroy, E. Muñoz, J.-L. Reverchon, Wide bandgap UV photodetectors: a short review of devices and applications, Gall. Nitride Mater. Devices II. 6473 (2007), http://dx.doi.org/10.1117/12.705393, 64730E.
[2] M.D.P. Corrêa, Solar ultraviolet radiation: properties, characteristics and amounts observed in Brazil and south America, An. Bras. Derm. Sifilogr. 90 (2015) 297–313, http://dx.doi.org/10.1590/abd1806-4841.20154089.
[3] A.A. Silva, Medidas de radiação solar ultravioleta em belo horizonte e saúde pública, Rev. Bras. Geofis. 26 (2008) 417–425, http://dx.doi.org/10.1590/s0102-261x2008000400003.
[4] W. Palz, Energia Solar E Fontes Alternativas, first ed., Hemus, Curitiba, 1995.

[5] Ş. Sağlam, Meteorological parameters effects on solar energy power generation, WSEAS Trans, Circuits Syst. 9 (2010) 637–649.
[6] H. Chen, K. Liu, L. Hu, A.A. Al-Ghamdi, X. Fang, New concept ultraviolet photodetectors, Mater. Today. 18 (2015) 493–502, http://dx.doi.org/10.1016/j.mattod.2015.06.001.
[7] D. Nunes, A. Pimentel, A. Goncalves, S. Pereira, R. Branquinho, P. Barquinha, E. Fortunato, R. Martins, Metal oxide nanostructures for sensor applications, Semicond. Sci. Technol. 34 (2019), http://dx.doi.org/10.1088/1361-6641/ab011e.
[8] A. Pimentel, A. Samouco, D. Nunes, A. Araújo, R. Martins, E. Fortunato, Ultra-fast microwave synthesis of ZnO nanorods on cellulose substrates for UV sensor applications, Materials (Basel). 10 (2017) 4–10, http://dx.doi.org/10.3390/ma10111308.
[9] R. Martins, E. Fortunato, P. Nunes, I. Ferreira, A. Marques, M. Bender, N. Katsarakis, V. Cimalla, G. Kiriakidis, Zinc oxide as an ozone sensor, J. Appl. Phys. 96 (2004) 1398–1408, http://dx.doi.org/10.1063/1.1765864.
[10] L. Peng, L. Hu, X. Fang, Low-dimensional nanostructure ultraviolet photodetectors, Adv. Mater. 25 (2013) 5321–5328, http://dx.doi.org/10.1002/adma.201301802.
[11] I.M. Costa, E.P. Bernardo, B.S. Marangoni, E.R. Leite, A.J. Chiquito, Metal to insulator transition in Sb doped SnO_2 monocrystalline nanowires thin films, J. Appl. Phys. 120 (2016), http://dx.doi.org/10.1063/1.4971870.
[12] J.M. Wu, C.H. Kuo, Ultraviolet photodetectors made from SnO_2 nanowires, Thin Solid Films 517 (2009) 3870–3873, http://dx.doi.org/10.1016/j.tsf.2009.01.120.
[13] Z. Ying, Q. Wan, Z.T. Song, S.L. Feng, SnO_2 nanowhiskers and their ethanol sensing characteristics, Nanotechnology 15 (2004) 1682–1684, http://dx.doi.org/10.1088/0957-4484/15/11/053.
[14] Y. Cheng, P. Xiong, C.S. Yun, G.F. Strouse, J.P. Zheng, R.S. Yang, Z.L. Wang, Mechanism and optimization of pH sensing using SnO_2 nanobelt field effect transistors, Nano Lett. 8 (2008) 4179–4184, http://dx.doi.org/10.1021/nl801696b.
[15] C. Wang, L. Yin, L. Zhang, D. Xiang, R. Gao, Metal oxide gas sensors: sensitivity and influencing factors, Sensors 10 (2010) 2088–2106, http://dx.doi.org/10.3390/s100302088.
[16] M.H. Jakob, B. Dong, S. Gutsch, C. Chatelle, A. Krishnaraja, W. Weber, M. Zacharias, Label-free SnO_2 nanowire FET biosensor for protein detection, Nanotechnology 28 (2017), http://dx.doi.org/10.1088/1361-6528/aa7015.
[17] O.M. Berengue, A.J. Chiquito, Direct evidence of traps controlling the carriers transport in SnO_2 nanobelts, J. Semicond. 38 (2017), http://dx.doi.org/10.1088/1674-4926/38/12/122001.
[18] H.W. Kim, S.H. Shim, Synthesis and characteristics of SnO2 needle-shaped nanostructures, J. Alloys. Compd. 426 (2006) 286–289, http://dx.doi.org/10.1016/j.jallcom.2006.01.093.
[19] H. Shi, B. Cheng, Q. Cai, X. Su, Y. Xiao, S. Lei, Surface state controlled ultrahigh selectivity and sensitivity for UV photodetectors based on individual SnO_2 nanowires, J. Mater. Chem. C Mater. Opt. Electron. Devices 4 (2016) 8399–8406, http://dx.doi.org/10.1039/c6tc02420c.
[20] D. Kim, G. Shin, J. Yoon, D. Jang, S.J. Lee, G. Zi, J.S. Ha, High performance stretchable UV sensor arrays of SnO_2 nanowires, Nanotechnology 24 (2013), http://dx.doi.org/10.1088/0957-4484/24/31/315502.
[21] J. Han, J. Lee, S. Ju, Fabrication of flexible ultraviolet photodetectors using an all-spray-coating process, AIP Adv. 6 (2016), http://dx.doi.org/10.1063/1.4948460.
[22] C.Y. Chen, M.W. Chen, C.Y. Hsu, D.H. Lien, M.J. Chen, J.H. He, Enhanced recovery speed of nanostructured ZnO photodetectors using nanobelt networks, IEEE J. Sel. Top. Quantum Electron. 18 (2012) 1807–1811, http://dx.doi.org/10.1109/JSTQE.2012.2200031.
[23] I.M. Costa, Y.N. Colmenares, P.S. Pizani, E.R. Leite, A.J. Chiquito, Sb doping of VLS synthesized SnO_2 nanowires probed by Raman and XPS spectroscopy, Chem. Phys. Lett. 695 (2018) 125–130, http://dx.doi.org/10.1016/j.cplett.2018.02.014.
[24] Y. Zou, Y. Zhang, Y. Hu, H. Gu, Ultraviolet detectors based on wide bandgap semiconductor nanowire: a review, Sensors (Switzerland). 18 (2018) 1–25, http://dx.doi.org/10.3390/s18072072.
[25] F. Kasten, A.T. Young, Revised optical air mass tables and approximation formula, Appl. Opt. 28 (1989) 4735, http://dx.doi.org/10.1364/ao.28.004735.
[26] G.J. McCarthy, J.M. Welton, X-ray diffraction data for SnO_2 an illustration of the new powder data evaluation methods, Powder Diffr. 4 (1989) 156–159, http://dx.doi.org/10.1017/S0885715600016638.
[27] M.O. Orlandi, E.R. Leite, R. Aguiar, J. Bettini, E. Longo, Growth of SnO nanobelts and dendrites by a self-catalytic VLS process, J. Phys. Chem. B 110 (2006) 6621–6625, http://dx.doi.org/10.1021/jp057099m.
[28] V.L. Rideout, A review of the theory and technology for ohmic contacts to group III-V compound semiconductors, Solid. Electron. 18 (1975) 541–550, http://dx.doi.org/10.1016/0038-1101(75)90031-3.
[29] A.J. Chiquito, C.A. Amorim, O.M. Berengue, L.S. Araujo, E.P. Bernardo, E.R. Leite, Back-to-back Schottky diodes: the generalization of the diode theory in analysis and extraction of electrical parameters of nanodevices, J. Phys. Condens. Matter 24 (2012), http://dx.doi.org/10.1088/0953-8984/24/22/225303.
[30] R. Dong, Y. Fang, J. Chae, J. Dai, Z. Xiao, Q. Dong, Y. Yuan, A. Centrone, X.C. Zeng, J. Huang, High-gain and low-driving-Voltage photodetectors based on organolead triiodide perovskites, Adv. Mater. 27 (2015) 1912–1918, http://dx.doi.org/10.1002/adma.201405116.
[31] T. Zhai, X. Fang, M. Liao, X. Xu, H. Zeng, B. Yoshio, D. Golberg, A comprehensive review of one-dimensional metal-oxide nanostructure photodetectors, Sensors 9 (2009) 6504–6529, http://dx.doi.org/10.3390/s90806504.
[32] A.L.R. Melzi, A.J. Chiquito, The interplay between Arrhenius and hopping conduction mechanisms in a percolating nanowire network, J. Phys. D Appl. Phys. 49 (2016), http://dx.doi.org/10.1088/0022-3727/49/31/315303.

Biographies

Estácio Paiva de Araújo is a Ph.D. candidate in Applied Physics at the Federal University of São Carlos, Brazil. He received his M.Sc. degree in Science of Materials Physics at the Federal University of Uberlândia, Brazil. His research interests include electronic transport phenomena, nanotechnology and bio-sensors.

Adryelle do Nascimento Arantes is a M.Sc. Candidate in physics at the Federal University of São Carlos, Brazil. She graduated in Medical Physics at the Federal University of Uberlândia, Brazil. Her research interets include electronic transport phenomena, nanotechnology and bio-sensors.

Ivani Meneses Costa is a post-doc associated researcher at Chemistry Institute - UNESP in Araraquara and at NanOLaB – UFSCar in São Carlos, Brazil. She received her Ph.D. degree in Applied Physics at the Federal University of São Carlos, Brazil. She received her M.Sc. degree in Applied Physics at the Federal University of Sergipe, Brazil. Her research interests are in the Condensed Matter Physics field, emphasizing in growth techniques, structural characterization, optical properties and electronic transport in nanostructured semiconductors.

Adenilson José Chiquito is a Professor at the Physics Department of the Federal University of São Carlos, Brazil. He received his post-doc degree in Physics at the São Paulo University, Brazil. He received his Ph.D. and M.Sc. degrees in Physics at the Federal University of São Carlos, Brazil. He is the head of NanOLaB laboratory at the Physics Department of the Federal University of São Carlos, Brazil. He has experience in electronic transport in low dimensional systems, optical and electrical properties of semiconductors.